DOI: 10.65322/j.srd.05192026.36

SPECTROSCOPIC AND THERMODYNAMIC STUDY OF THE MOLECULAR INTERACTION BETWEEN SILK SERICIN AND MIMOSA CONDENSED TANNINS

Tuxliyev G'.A.,
E-mail: gayratalituxliyev@gmail.com
Namangan State Technical University

Abstract. *This study evaluates the interaction between silk sericin and mimosa condensed tannins using UV-Vis difference spectroscopy, fluorescence quenching, van't Hoff analysis and FTIR at pH 7.4. Between 293 and 313 K, the Stern–Volmer constant decreased from 1.65×10^4 to 1.05×10^4 M^{-1}. The apparent binding parameter was 1.18×10^5 M^{-1} at 293 K; apparent enthalpy and entropy were −42.2 kJ/mol and −46.9 J/(mol·K). FTIR fitting indicated an increase in β-sheet content from 32% to 55%. These observations are consistent with association and structural reorganisation. However, molecular heterogeneity and model assumptions limit the interpretation of binding parameters; exact stoichiometry and collagen bridging require independent verification.*

Annotatsiya. *Tadqiqotning maqsadi ipak seritsini va mimozaning kondensatsiyalangan tanninlari o'rtasidagi o'zaro ta'sirni baholashdir. pH 7,4 da UV-Vis farq spektroskopiyasi, fluoresensiyaning so'nishi, van't Hoff tahlili va FTIR usullari qo'llangan. 293–313 K oralig'ida Stern–Volmer konstantasi $1,65\times10^4$ dan $1,05\times10^4$ M^{-1} gacha kamaygan. Hisoblangan ko'rinma bog'lanish parametri 293 K da $1,18\times10^5$ M^{-1} ni tashkil etgan; ko'rinma entalpiya va entropiya mos ravishda −42,2 kJ/mol va −46,9 J/(mol·K) bo'lgan. FTIR tahlilida β-qatlam ulushi 32 foizdan 55 foizgacha oshgan. Natijalar kompleks hosil bo'lishi va tuzilish o'zgarishlariga mos keladi, ammo aniq stexiometriya hamda kollagen bilan bog'lanishni mustaqil sinovlar bilan tekshirish zarur.*

Аннотация. *Цель исследования — оценить взаимодействие серицина шёлка с конденсированными таннинами мимозы. При pH 7,4 использованы разностная УФ-видимая спектроскопия, тушение флуоресценции, анализ Вант-Гоффа и ИК-Фурье-спектроскопия. В диапазоне 293–313 K константа Штерна–Фольмера снизилась с $1,65\times10^4$ до $1,05\times10^4$ M^{-1}. Кажущийся параметр связывания при 293 K составил $1,18\times10^5$ M^{-1}; кажущиеся энтальпия и энтропия — −42,2 кДж/моль и −46,9 Дж/(моль·K). Доля β-структуры по данным ИК-анализа возросла с 32 до 55 %. Результаты согласуются с комплексообразованием и структурной перестройкой, однако точная стехиометрия и связывание с коллагеном требуют независимой проверки.*

Keywords: *silk sericin; condensed tannins; protein–polyphenol interaction; fluorescence quenching; FTIR; binding thermodynamics.*

Kalit so'zlar: *ipak seritsini; kondensatsiyalangan tanninlar; oqsil–polifenol o'zaro ta'siri; fluoresensiya so'nishi; FTIR; bog'lanish termodinamikasi.*

Ключевые слова: *серицин шёлка; конденсированные таннины; взаимодействие белок–полифенол; тушение флуоресценции; ИК-Фурье-спектроскопия; термодинамика связывания.*

Introduction

Protein-polyphenol interactions affect astringency and the properties of biological materials [1, 2]. Plant polyphenols can stabilise collagen [3], while condensed tannins are established vegetable tanning agents [4]. Sericin is a hydrophilic silk protein fraction with potential applications in biomaterials and substantial molecular heterogeneity [5–7]. Recovery from silk-processing wastewater provides a possible source of this material [8].

DOI: 10.65322/j.srd.05192026.36

This study assesses sericin–mimosa association, temperature-dependent fluorescence quenching and FTIR structural changes. Leather-processing applications are considered as hypotheses requiring direct validation.

Materials and methods

Sericin was recovered from cocoon degumming wastewater supplied by JSC "Bukhoro-Pillakorlik" through acid-isoelectric precipitation at pH 4.2 and 5 °C. The lyophilised material had a reported protein content of 89.4 ± 1.0% (Kjeldahl, N×6.25), residual sugar content of 3.6% and an SDS-PAGE molecular-mass range of 35–80 kDa. Mimosa extract from Tanac S.A. contained 65 ± 2% condensed tannin and had a reported weight-average molecular mass of 1280 Da by gel permeation chromatography. Solutions used 10 mM phosphate buffer, pH 7.4 ± 0.05, and 18 MΩ·cm water.

Concentrations below retain the nominal molar scale of the supplied dataset. The effective sericin molecular mass used for conversion and correction for protein/tannin purity were not specified. Consequently, association constants and molar ratios are treated as apparent quantities rather than uniquely defined molecular properties.

UV-Vis difference spectra were recorded at 25 °C with a Specord 250 Plus instrument and 1.0 cm quartz cuvettes. Nominal sericin concentration was 20 μM, with tannin at 0–150 μM; the reported titration increment was 1 μM. A tannin-only reference of equivalent concentration was used. Spectra were baseline-corrected in Origin 2023.

Fluorescence was measured with a Cary Eclipse instrument at 275 nm excitation and 5 nm excitation/emission slits. Sericin (5 μM) was titrated with 0, 5, 10, 20, 40, 60, 80 and 100 μM tannin at 293, 303 and 313 K; temperature control was ±0.1 °C. Measurements were reported in triplicate. Inner-filter correction and the Stern–Volmer relationship were applied as follows [9, 10]:

$$F_{corr} = F_{obs} \times 10^{(A_{ex} + A_{em})/2} \quad (1)$$

$$F_0/F = 1 + K_{SV}[Q]; \quad k_{q,app} = K_{SV}/\tau_0 \quad (2)$$

Here A_{ex} and A_{em} are sample absorbances at excitation and emission wavelengths; [Q] is nominal tannin concentration. The lifetime $\tau_0 = 5\times10^{-9}$ s was assumed, not measured, consistently with the reported kq values. Thus kq,app is a diagnostic estimate, not a measured collisional rate constant. Empirical double-logarithmic fits were retained:

$$log_{10}[(F_0 - F)/F] = log_{10} K_{app} + n_{app}\, log_{10}[Q] \quad (3)$$

The slope n_{app} is an empirical exponent, not an independently measured number of binding sites [11]. Numerical intercepts depend on the concentration convention and the assumed binding model. Apparent thermodynamic quantities were estimated using [12]:

$$ln\, K_{app} = -\Delta H_{app}/(RT) + \Delta S_{app}/R \quad (4)$$

$$\Delta G_{app} = \Delta H_{app} - T\Delta S_{app} = -RT\, ln\, K_{app} \quad (5)$$

For this formal calculation, the numerical molar concentration convention corresponds to a 1 M standard state. Interpretation as standard molecular binding thermodynamics requires a validated equilibrium model. R = 8.314 J/(mol·K).

FTIR spectra were recorded with a Shimadzu IRAffinity-1S using KBr pellets, 32 scans and 4 cm^{-1} resolution. Complexes at nominal sericin:tannin ratios of 1:3, 1:5 and 1:10 were incubated for 60 min at 25 °C and lyophilised. The 1700–1600 cm^{-1} region was baseline-corrected and fitted with Gaussian components in Peakfit v4.12; reported reconstruction R^2 was ≥0.998. Amide-I analysis follows the general approach of Byler and Susi [13].

Results

UV-Vis spectra showed hypochromism near 275 nm, a shift towards 282 nm and an intersection near 281 nm at A = 0.72 (Fig. 1). The supplied titration curve gave Kd,app ≈35 μM. These features are consistent with changing association, but the intersection alone does not establish exactly two chemical species or exclude aggregation.

DOI: 10.65322/j.srd.05192026.36

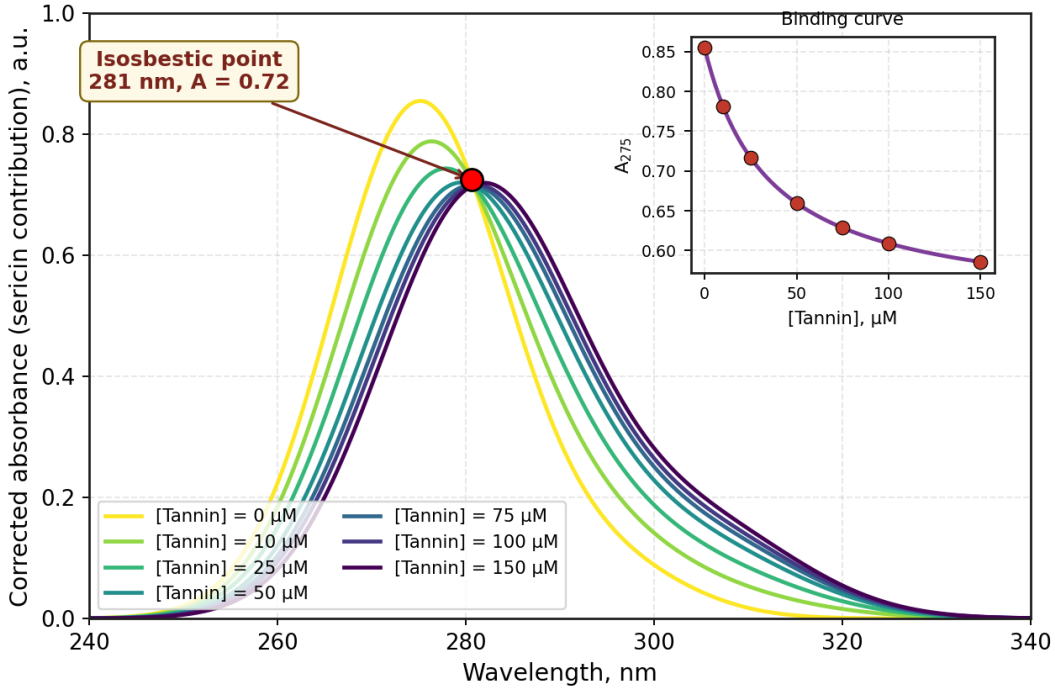

Fig. 1. UV-Vis difference spectra at pH 7.4 and 298 K; nominal sericin concentration 20 μM

Fluorescence decreased with increasing tannin concentration (Fig. 2). K_{sv} declined from 1.65×10^4 to 1.05×10^4 M^{-1} over 293–313 K. The reported double-logarithmic parameters and thermodynamic estimates are summarised in Tables 1 and 2.

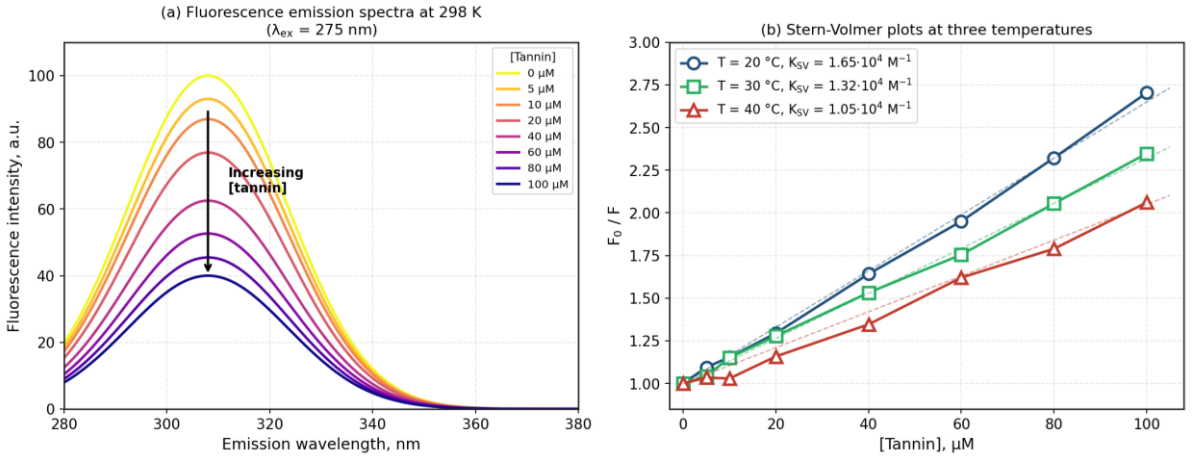

Fig. 2. Fluorescence spectra and Stern–Volmer plots on the reported concentration scale

Table 1

Reported fluorescence fit parameters (three measurements; mean ± SD)

T (K)	K_{sv} / 10^4 M^{-1}	kq,app / 10^{12} L mol^{-1} s^{-1}	K_{app} / 10^4 M^{-1}*	n_{app}
293 (20 °C)	1.65 ± 0.04	3.30	11.80 ± 0.42	1.05 ± 0.02
303 (30 °C)	1.32 ± 0.03	2.64	6.70 ± 0.28	1.04 ± 0.02
313 (40 °C)	1.05 ± 0.03	2.10	3.90 ± 0.18	1.03 ± 0.02

DOI: 10.65322/j.srd.05192026.36

*K_{app} retains the original molar reporting convention; n_{app} is an empirical slope. Uncertainty in the assumed lifetime is not included in kq,app.

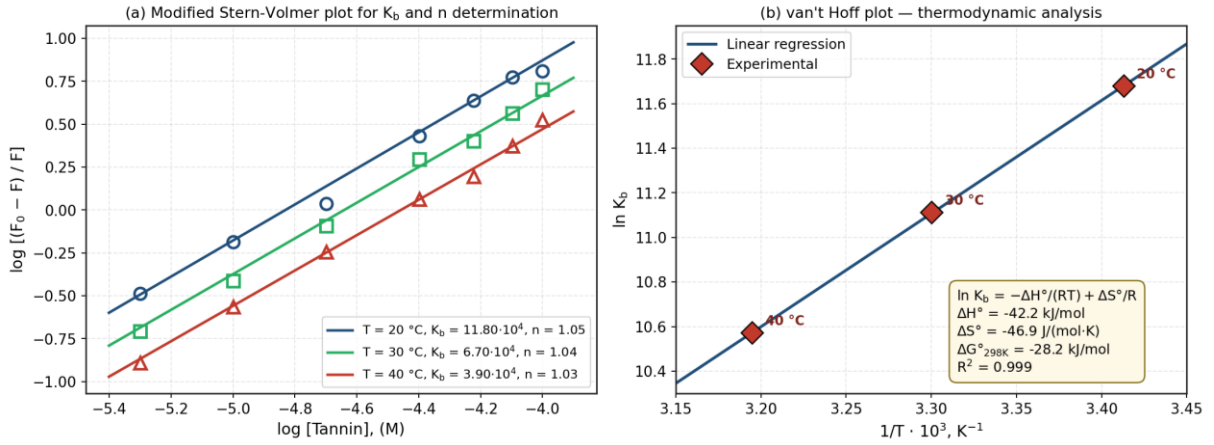

Fig. 3. Reported double-logarithmic fits and van't Hoff analysis

Table 2

Reported apparent thermodynamic estimates; uncertainties retained from the source

Parameter	293 K	303 K	313 K
ΔG_{app} (kJ/mol)	−28.4 ± 0.3	−28.0 ± 0.3	−27.5 ± 0.3
ΔH_{app} (kJ/mol)	−42.2 ± 0.7	−42.2 ± 0.7	−42.2 ± 0.7
ΔS_{app} (J mol^{-1} K^{-1})	−46.9 ± 1.2	−46.9 ± 1.2	−46.9 ± 1.2
$T\Delta S_{app}$ (kJ/mol)	−13.7	−14.2	−14.7

The tabulated K_{app} values reproduce ΔH_{app} ≈−42.2 kJ/mol and ΔS_{app} ≈−46.9 J/(mol·K). At 298 K, $T\Delta S_{app}$ ≈−14.0 kJ/mol and $-T\Delta S_{app}$ ≈+14.0 kJ/mol, giving ΔG_{app} ≈−28.2 kJ/mol. This arithmetic agreement does not independently validate the underlying binding model.

The FTIR decomposition indicated increasing β-sheet fractions of 32%, 40%, 48% and 55% for sericin and the 1:3, 1:5 and 1:10 mixtures, respectively (Fig. 4). Random-coil fractions decreased from 48% to 28%. The original figure assigns 15% β-turn to pure sericin and 14% to the mixtures; α-helical contributions remain small.

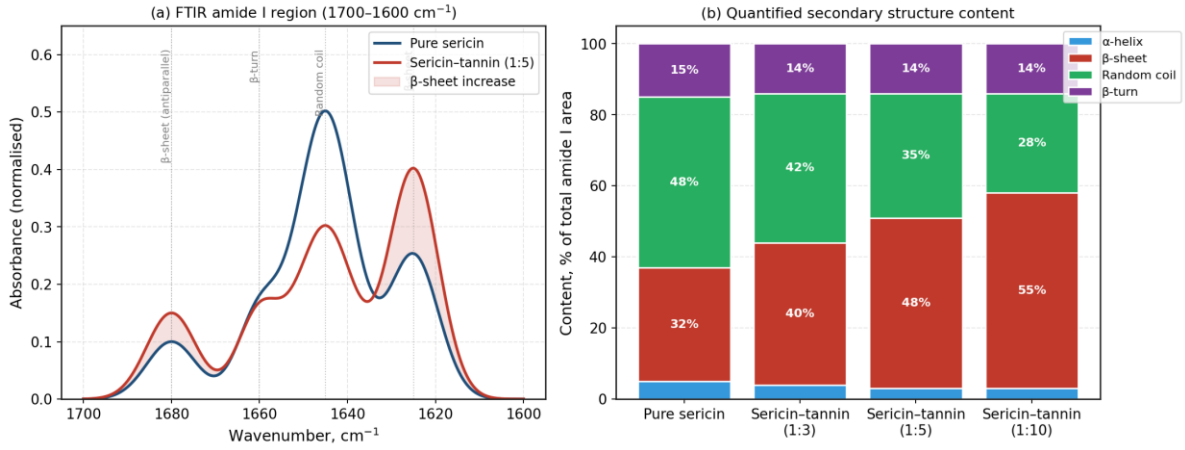

Fig. 4. Amide-I spectra and reported secondary-structure fractions in lyophilised samples

DOI: 10.65322/j.srd.05192026.36

Analysis

UV-Vis Kd,app ≈35 μM differs from $1/K_{app}$ ≈8.5 μM at 293 K (approximately 11.4 μM at 298 K using the fitted temperature dependence). Temperature therefore does not fully account for the discrepancy. Distinct observables, concentration conventions and model assumptions should be examined before assigning a unique affinity.

There is also an internal consistency issue between the two fluorescence fits. At 293 K and [Q] = 100 μM, equation (2) gives F_0/F ≈2.65, whereas equation (3), using $K_{app} = 1.18\times10^5$ and n_{app} = 1.05, gives F_0/F ≈8.45. The supplied constants are retained for traceability, but the raw titration data require joint reanalysis before these fits can be regarded as mutually consistent.

Discussion

The decreasing K_{sv} and large kq,app are compatible with a static contribution, but lifetime-resolved measurements and checks for scattering and aggregation are needed to distinguish mechanisms. Negative apparent enthalpy and entropy are compatible with hydrogen bonding and van der Waals contributions [12]; they do not uniquely identify all interacting forces in a heterogeneous mixture. Protein–polyphenol association and precipitation are composition-dependent [14].

FTIR changes support altered dry-state spectral composition, but tannin-band overlap, lyophilisation and fitting choices may influence the assigned secondary-structure fractions. High reconstruction R^2 alone does not quantify structural uncertainty. The reported triplicates also do not establish whether independent sample preparations were tested; regression confidence intervals and the propagation of concentration uncertainty remain unavailable.

Sericin-assisted vegetable tanning warrants further study. Collagen bridging, industrial saturation, leather performance and dissociation above 60 °C were not tested and remain hypotheses requiring direct validation.

Conclusion. The reported spectra are consistent with sericin–tannin association. Although the van't Hoff calculation reproduces the tabulated estimates, inconsistent fluorescence fits prevent firm affinity or stoichiometry claims. Raw-data reanalysis, a defined molar concentration basis and independent mechanism controls are required before leather-processing applications can be assessed.

References

1 Brossaud, F., Cheynier, V., & Noble, A. C. (2001). Bitterness and astringency of grape and wine polyphenols. Australian Journal of Grape and Wine Research, 7(1), 33–39.

2 Quideau, S., Deffieux, D., Douat-Casassus, C., & Pouységu, L. (2011). Plant polyphenols: Chemical properties, biological activities, and synthesis. Angewandte Chemie International Edition, 50(3), 586–621.

3 Madhan, B., Subramanian, V., Rao, J. R., Nair, B. U., & Ramasami, T. (2005). Stabilization of collagen using plant polyphenol: Role of catechin. International Journal of Biological Macromolecules, 37(1–2), 47–53.

4 Falcão, L., & Araújo, M. E. M. (2018). Vegetable tannins used in the manufacture of historic leathers. Molecules, 23(5), 1081.

5 Aramwit, P., Siritientong, T., & Srichana, T. (2012). Potential applications of silk sericin, a natural protein from textile industry by-products. Waste Management & Research, 30(3), 217–224.

6 Takasu, Y., Yamada, H., & Tsubouchi, K. (2002). Isolation of three main sericin components from the cocoon of the silkworm, Bombyx mori. Bioscience, Biotechnology, and Biochemistry, 66(12), 2715–2718.

7 Lamboni, L., Gauthier, M., Yang, G., & Wang, Q. (2015). Silk sericin: A versatile material for tissue engineering and drug delivery. Biotechnology Advances, 33(8), 1855–1867.

DOI: 10.65322/j.srd.05192026.36

8 Capar, G., Aygun, S. S., & Gecit, M. R. (2008). Treatment of silk production wastewaters by membrane processes for sericin recovery. Journal of Membrane Science, 325(2), 920–931.

9 Lakowicz, J. R. (2006). Principles of fluorescence spectroscopy (3rd ed.). Springer.

10 Eftink, M. R., & Ghiron, C. A. (1981). Fluorescence quenching studies with proteins. Analytical Biochemistry, 114(2), 199–227.

11 Lissi, E., Calderón, C., & Campos, A. (2013). Evaluation of the number of binding sites in proteins from their intrinsic fluorescence: Limitations and pitfalls. Photochemistry and Photobiology, 89(6), 1413–1416. https://doi.org/10.1111/php.12112

12 Ross, P. D., & Subramanian, S. (1981). Thermodynamics of protein association reactions: Forces contributing to stability. Biochemistry, 20(11), 3096–3102.

13 Byler, D. M., & Susi, H. (1986). Examination of the secondary structure of proteins by deconvolved FTIR spectra. Biopolymers, 25(3), 469–487.

14 Hagerman, A. E., & Butler, L. G. (1981). The specificity of proanthocyanidin–protein interactions. Journal of Biological Chemistry, 256(9), 4494–4497.